

Radionuclide analysis in the soil of Kumaun Himalaya, India, using gamma ray spectrometry

R. C. Ramola^{1*}, V. M. Choubey², Ganesh Prasad¹, G. S. Gusain¹, Z. Tosheva³ and A. Kies³

¹Department of Physics, H. N. B. Garhwal University, Badshahi Thaul Campus, Tehri Garhwal 249 199, India

²Wadia Institute of Himalayan Geology, Dehradun 248 001, India

³Laboratoire Physique des Radiations, Université du Luxembourg, 162A avenue de la Faiencerie, L-1511 Luxembourg

Environmental release of low levels of radioactivity can occur as a consequence of normal radionuclides present in the earth's crust. We present here the results of a survey undertaken in 2003 on the radionuclide concentration in different rock formations in the eastern part of Kumaun Himalaya. The activity concentration and gamma-absorbed dose rates of the terrestrial radionuclides caused by ²²⁶Ra, ²³²Th and ⁴⁰K were determined in the soil samples collected from the eastern part of Kumaun Himalaya. The mean concentration of ²³⁸U and ²³²Th in the earth's crust varied from 0.5 to 5 ppm (6 to 60 Bq/kg) and 2 to 20 ppm (8 to 80 Bq/kg) respectively. The reported activity concentration for the different rock formations varied from 32.6 to 1305.5 Bq/kg for ²³⁸U, 16.3 to 136.3 Bq/kg for ²³²Th and 124.6 to 1758.0 Bq/kg for ⁴⁰K. The distribution of the radionuclides varied with rock type due to different chemical properties of the measured radionuclides and the rocks. The result shows that high activity levels were found in Saryu Formation consisting of augen-gneiss, granite interbedded with schists and flaggy quartzite. The total air-absorbed dose rate in air above 1 m height was calculated from the three radionuclides (²²⁶Ra, ²³²Th and ⁴⁰K), which varied from 39.1 to 226.8 nGy h⁻¹. The internal and external health-hazard indices were calculated based on the concentration of ²²⁶Ra, ²³²Th and ⁴⁰K. Strong positive correlations were observed between ²³⁵U and ²²⁶Ra, ²³²Th and ²²⁶Ra, ⁴⁰K and ²³²Th as well as ⁴⁰K and ²²⁶Ra. However, no significant correlation was observed between ²³⁸U and ²²⁶Ra because of radioactive disequilibrium between them.

Keywords: Dose rate, external hazard index, geological formations, radionuclides.

THE principal origins of ionizing radiation exposure are natural sources. The spatial distribution of natural radiation is highly variable and dependent on the local geologic formations¹. The levels of radioactivity in water and soil are important mainly because of two principal radiological effects. The first is the external irradiation of the body by gamma rays emitted from radionuclides present

in the area, and the second is internal irradiation of lung by alpha-emitting, short-lived decay products of radon and thoron¹⁻³. The average crustal abundances of uranium and thorium are 1.8 and 7.2 ppm (ref. 4). In igneous rocks, uranium concentration increases with the degree of delineation; very low uranium concentrations occur in ultrabasic rocks (0.014 ppm) and higher concentrations in granites (2–15 ppm)^{5,6} and pegmatites. Guthrie and Kleeman⁷ studied changing uranium distribution in deuterically altered granite during weathering. Waite and Payne⁸ found that oxidation and other types of alteration altered the primary uranium minerals chemically, such as uraninite producing uranyl silicates. Guthrie and Kleeman⁷ observed no net loss of uranium in moderately weathered granites, but that profound weathering resulted in mobilization of uranium. Langmuir and Herman⁹ observed that thorium in rocks is found at similar sites as those of uranium, zircon and other minerals. In metamorphic rocks, the uranium and thorium abundances and distributions are dependent on the source rock⁶. Higher uranium concentrations are also associated with deposits that contain heavy minerals, such as placer deposits¹⁰. Radium isotopes are produced by the decay of ²³⁸U, ²³⁵U and ²³²Th. The presence of radium is not affected by long-term processes, due to its continuous production and relatively short half-life¹¹, but the disequilibrium between ²³⁸U and ²²⁶Ra is often observed as a result of different mobilities in soil, rock and aquifers.

The natural radioactivity of soil samples is usually determined from the ²²⁶Ra, ²³²Th and ⁴⁰K contents¹². Due to the spatial variation in external gamma dose rate, it is essential to measure the radionuclide content in surrounding soil samples. These doses vary depending upon the concentrations of the natural radionuclides, ²³⁸U, ²³²Th, their daughter products and ⁴⁰K, present in the soils and rocks, which in turn depend upon the local geology of each region in the world^{13,14}. Nation-wide surveys have been carried out to determine natural radionuclides, radium equivalent activity and the resulting doses^{3,15-18}.

Studies in the Himalayan region have shown that the tectonic processes, types of rocks and geohydrological characteristics of rock mass control the concentration of radon in soil and water¹⁹. The aim of the present study was to find out the variation of radionuclides in different lithotectonic units in the eastern part of Kumaun Himalaya. The role of various rock types and associated tectonic features was also considered in the interpretation of distribution of radionuclides. This communication also presents the argument about distribution of radionuclides and interpretation of data and their relation to the internal and external hazard indices in the study area for the general public.

The study area lies in the eastern part of Kumaun Himalaya. The geology of the area has been studied in detail by a number of workers²⁰⁻²³. The study area falls in the subtropical Lesser Himalayan belt in the eastern part

*For correspondence. (e-mail: rcramola@gmail.com)

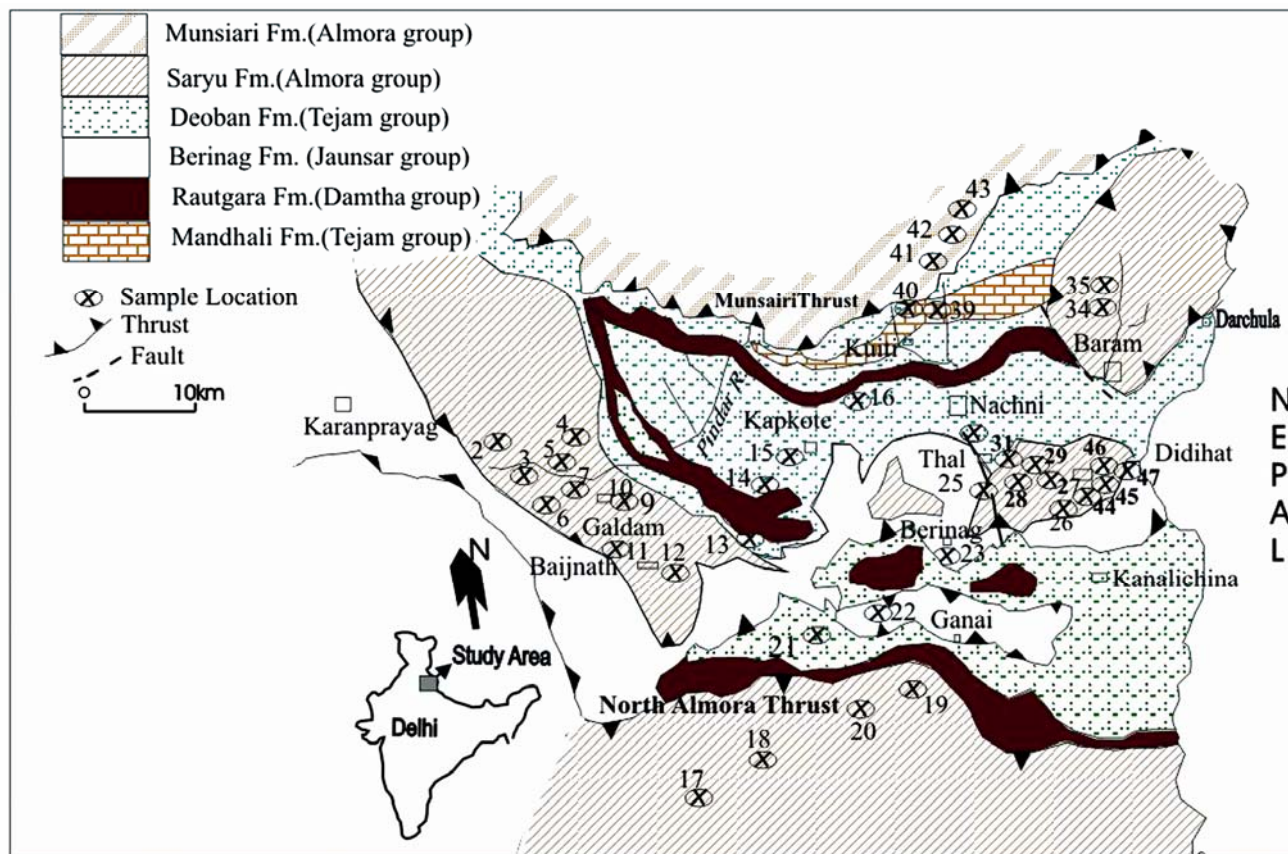


Figure 1. Geological map of the eastern part of Kumaun Himalaya showing soil sample location.

of Kumaun Himalaya. In general, the rocks are characterized by multiple deformations resulting in superimposed folding and repeated faulting and thrusting. The rocks exposed in the area, from south to north, belong to the Saryu Formation of Almora Group (sericite–chlorite schist, amphibolite, mylonitized granite gneiss, augen gneiss with schist and intruded granite, garnetiferous mica schist and micaceous weathered quartzite, and granodiorite in the Champawat area), Rautgara Formation (muddy quartzite and green–purple slates), Deoban Formation (predominantly dolomitic limestone, slates and phyllites), Mandhali Formation (pyretic slates, argillaceous and dolomitic limestone) and Berinag Formation (massive white, pale, purple and green quartzite with metamorphosed basalt and tuffites). The Berinag Thrust separates the rocks of Berinag Formation from Deoban Formation, whereas rocks of the Berinag Formation are separated from the Saryu Formation (granites, gneisses and porphyrites) in the Askot area by the Askot Thrust. In the northern part, the Deoban and Rautgara formations are separated from the Saryu Formation by the Chiplakot Thrust. The meso-to-epi grade para and orthogneisses, schist, calc-silicate, marble, granites and their mylonitic equivalent form the Munsiri Formation, which constitutes the root zone rocks of the far-travelled detached

pieces (nappe and klippe) in the Lesser Himalaya. The Munsiri Thrust separates the rocks of the Saryu Formation from the underlying Deoban Formation (Figure 1).

The soil samples were collected from a depth of 60 cm in 1000 ml plastic beakers, keeping in view that the top layer soil is removed by leaching process. After collection, under laboratory conditions, organic material, pebbles, roots and vegetation were separated from the soil sample and all samples were crushed in small lumps mechanically. Then the samples were fully dried in an electric furnace at 110°C, for about a day. Then dried samples were converted into fine powder using an automatic crusher, homogenized and sieved. The 150 µm mesh size fraction of the sample was used for the present study. The prepared samples were transferred to the standard 500 ml Marinelli beakers that were hermetically sealed for the uniform distribution of ^{220}Rn and ^{222}Rn daughter products in the soil samples to ignore any accumulation on the surface of the soil. The containers were stored for a period of one month before gamma spectrometric analysis, so as to allow the establishment of secular equilibrium between ^{226}Ra , ^{232}Th and their daughter products^{24–27}. Prior to measurement of the samples, the environmental gamma background at the laboratory site was determined with an empty cylindrical Marinelli

beaker under identical conditions. The containers were placed coaxially with the detector for determination of efficiency and the same geometry was used for the sample and background measurements. It was later subtracted from the measured gamma-ray spectra of each sample.

Gamma spectroscopy was used for the measurement of specific activity of the soil samples, as this is a non-destructive method and provides information for almost all natural radionuclides of interest due to its excellent separation capabilities. Other advantages are that it is a less time-consuming method compared to chemical methods and cheaper compared to the new methods like mass spectrometry.

High purity germanium (HPGe) detector was used for the measurement of specific activity of the soil samples due to its excellent properties such as: (i) lower impurity concentration and (ii) greater axial uniformity of the impurity concentration over several centimetres. The measurements were made with Be window and p-type HPGe top detectors with specifications 45% and 43% relative efficiency and resolution of 0.67/1.8 and 0.8/1.87 keV for 122 and 1332 keV peaks respectively. The detector was cooled down by liquid nitrogen, and its warm-up sensor was coupled to the high-voltage detector bias supply, which was equipped with a remote shutdown feature. The signals were processed by the main amplifier incorporated with an efficient pile-up rejector and a multi-channel buffer consisting of an analogue-to-digital converter. An advanced multi-channel analyser with MAESTRO-32 software enabled data acquisition, storage, display and online analysis of the acquired gamma spectra. The shielding was made of Pb, Cu and Cd, which was able to suppress the background gamma radiation present at the laboratory site. The energy calibration of the detector was done with the help of the source of ^{133}Ba , ^{137}Cs and ^{60}Co . The efficiency calibration for the system was carried out using secondary standard source of uranium ore in geometry available for sample counting. Efficiency values were plotted against energy for a particular geometry and fitted by least square method to an empirical relation that takes into account the nature of the efficiency curve for the HPGe detector. The efficiency calibration was cross-checked by the certified reference materials (IAEA-314) obtained from AQCS/IAEA, Austria²⁸. All measurements of the samples, background and standards were done in the same sample to detector geometry for 24 h.

The offline analysis of each gamma ray spectrum was carried out by a dedicated software program (Gamma Vision-32), which performs a simultaneous fit and multiple peak de-convolution to all the statistically significant photo-peaks appearing in the spectrum. A menu-driven report gave information about centroid channel, energy, background counts, net area counts, width of identified and unidentified peaks, and intensity and mean activity of

the radionuclides present in the sample and the standard deviation. Activity concentration of ^{232}Th radionuclide was determined from the average concentrations of short-lived daughter radionuclides ^{212}Pb and ^{228}Ac (238.6 and 911.1 keV). ^{238}U was determined from the average concentration of ^{214}Pb and ^{214}Bi (351.9 and 609.3 keV) using general practices^{29,30}. To assess the isotopic composition of uranium in soil samples the overlapping gamma emissions from different nuclides have to be identified and resolved²⁴. Since ^{238}U does not emit suitable gamma rays which can be directly measured using gamma ray spectrometry, it is usually determined through its daughter products in equilibrium. Thorium-234 has a short half-life (24.1 d) and mean life (34.7 d) and so comes into secular equilibrium with ^{238}U and emits low-energy photons with low yield at the energies 63.29 keV (3.8%), 92.35 keV (2.72%) and 92.78 keV (2.69%). The multiple photo-peaks from the latter two energy photons cannot be resolved easily, and so the 63.29 keV peak was used for the determination of ^{238}U . In the present work, the $^{234\text{m}}\text{Pa}$ was not used to derive ^{238}U activity from the soil samples because of its short half-life (6.7 h); also, it is always in equilibrium with its parent ^{234}Th and emits 1001.03 keV photons with very low yield (0.837%)²⁵. The determination of ^{235}U was difficult because it emits several photons; the only photons that can be used for the determination of ^{235}U are those at the energy of 185.72 keV. The common approach for the subtraction of the contribution of the 186 keV line from the ^{238}U series was used for the determination of ^{235}U activity. ^{226}Ra activity can be derived indirectly from the weighted average of the activities of two photo-peaks of ^{214}Pb (295.2 and 352.0 keV) and three photo-peaks of ^{214}Bi (609.3, 1120.3 and 1764.5 keV), and directly from the 186.25 keV photons. These two methods agree within the total uncertainty of the measurements³¹. Here the intense gamma rays of ^{214}Pb and ^{214}Bi were used for the determination of ^{226}Ra activity²⁴. However, true measurement of ^{40}K and ^{137}Cs concentrations was made by their own gamma rays at 1460.8 and 661.6 keV respectively. The specific activity of *i*th nuclide from the respective energy peak can be calculated by the following formula:

$$A_i = N_E / (t \gamma \varepsilon M), \quad (1)$$

where N_E is the net peak area of a peak at energy E , ε the detection efficiency at energy E , t the counting live-time, γ the gamma-ray yield per disintegration of the specific nuclide for a transition at energy E , and M the mass (kg) of the measured sample. For more than one peak having the same energy range of analysis, the peak activities were averaged and the resulting weighted average gave the activity of the nuclide. The uncertainties arise due to a number of factors like volume of the samples, type-B-like calibration, peak area determination and sample counts. The combined uncertainties of all these factors did not

exceed 7–8% for ^{226}Ra and ^{232}Th . The combined uncertainties for ^{40}K were about 20% due to the contribution of ^{228}Ac at 1459.2 keV with gamma-ray line of ^{40}K in the same region. To validate this method, the certified reference samples (IAEA-312 and 313) of known activities were measured^{28,32}. The HPGe detector has a thin Be window which is more sensitive to the coincidences and uncertainties of approximately same energy lines. To minimize the uncertainties only isolated gamma lines were analysed and measurements were repeated at least twice for a single sample. The low level detection for ^{226}Ra , ^{232}Th and ^{40}K was calculated from the Currie³³ formula to be 1.1, 1.0 and 8.2 Bq/kg respectively.

Based on the measured values of ^{226}Ra , ^{232}Th and ^{40}K , the radium equivalent activity for all soil samples under study was calculated using the relation^{16,34,35}

$$\text{Ra}_{\text{eq}} = A_{\text{Ra}} + 1.43A_{\text{Th}} + 0.077A_{\text{K}}, \quad (2)$$

where A_{Ra} , A_{Th} and A_{K} are the activity concentrations of ^{226}Ra , ^{232}Th and ^{40}K in Bq/kg respectively.

Local stones and soil are used for the construction of houses in the hilly areas. It is expected that the radiation dose would be delivered externally, if a building is constructed using local rocks/soil. The external hazard index (H_{ex}) and internal hazard index (H_{in}) were calculated by the following equation^{18,36,37}:

$$H_{\text{ex}} = A_{\text{Ra}}/370 + A_{\text{Th}}/259 + A_{\text{K}}/4810, \quad (3)$$

$$H_{\text{in}} = A_{\text{Ra}}/185 + A_{\text{Th}}/259 + A_{\text{K}}/4810. \quad (4)$$

The outdoor air-absorbed dose rates due to terrestrial gamma rays at 1 m above the ground were calculated from ^{226}Ra , ^{232}Th and ^{40}K concentrations in the soil assuming that the contribution of other radionuclides to the environmental background was negligible^{18,38,39}. The absorbed dose rates were calculated by the conversion factor⁴⁰:

$$D = 0.461A_{\text{Ra}} + 0.623A_{\text{Th}} + 0.0414A_{\text{K}}. \quad (5)$$

For the above calculation the decay products of ^{226}Ra and ^{232}Th are considered in equilibrium. Finally in order to calculate the annual effective dose rate due to the presence of ^{226}Ra , ^{232}Th and ^{40}K in soil samples, one has to take into account the conversion coefficient from absorbed dose in air to effective dose and the indoor occupancy factor¹.

Ambient dose equivalent rate (mSv y^{-1}) = Dose rate in (nGy h^{-1}) (24 h) \times 365.25d \times 0.8 (indoor occupancy factor) \times 0.7 Sv Gy^{-1} (conversion coefficient) $\times 10^{-6}$.

Based on the analysis in the UNSCEAR report⁴¹, a coefficient of 0.7 Sv Gy^{-1} was used to convert the absorbed dose in air to effective dose equivalent and the indoor occupancy factor was assumed to be 0.8, implying that

20% of time is spent outdoors on an average around the world.

The distribution of radionuclides and their isotopic fraction are summarized in Table 1. The sample locations are shown in Figure 1. The results of 37 soil samples collected from different lithotectonic units in the eastern part of Kumaun Himalaya are discussed here. The data were collected from five different formations of the study area. In general, soil thickness in the study area is small (0.5 m to a maximum of 2 m) because of the rugged topography and fast erosion along the slopes¹⁵. Therefore different horizon studies (with varying depths) for the radionuclides are not possible in the study area. The radionuclide concentration in the soil samples directly reflects the concentration of radionuclides in the underlying rock at equilibrium.

The discussion here has been divided into four parts, i.e. radionuclide distribution, radium equivalent activity, hazard index and air-absorbed dose rate. These results show that the radionuclides are extensively affected by soil-formation processes. The activity of ^{40}K (124.6–1758 Bq/kg), ^{238}U (32.6–1305.5 Bq/kg), ^{235}U (1.2–18.2 Bq/kg), ^{226}Ra (2.4–186.9 Bq/kg), ^{232}Th (16.3–136.3 Bq/kg), ^{230}Th (0.2–11.5 Bq/kg), ^{210}Pb (0.1–260.6 Bq/kg) and ^{137}Cs (0.4–8.2 Bq/kg) was measured (Table 2), but more emphasis will be given to discussion of the results of ^{226}Ra , ^{232}Th and ^{40}K . For this the data have been divided according to five different rock formations for easy interpretation of external hazard index and dose calculation in a small region. The mean values of ^{226}Ra , ^{232}Th and ^{40}K in soil samples with 95% confidence level for different formations are given in Table 3. The highest levels of these radionuclides were recorded in the Saryu Formation. The variations of radioactivity levels at different measurement locations are due to the variation of concentration of these radioactive elements in the geological formations, and micro-cracks and defects in the rocks. Micro-cracks and defects provide a tunnel for the upward movement of radionuclides and enhance the radioactivity level. ^{137}Cs was recorded the highest in Deoban Formation of the study area. The radioactive related minerals such as zircon, iron oxides and fluorite play an important role in controlling the distribution of uranium and thorium. Zircon usually contains uranium and thorium concentration ranging from 0.01% to 0.19% and 1% to 2% respectively⁴².

The activity of ^{226}Ra in sedimentary rocks of Berinag Formation, predominantly dominated by quartzite rocks, varied from 2.4 to 28.2 Bq/kg with a mean value of 15.3 Bq/kg. The activity of ^{40}K was 155.4–429.1 Bq/kg, with a mean value of 292.3 Bq/kg. The radium equivalent activity in this formation varied from 110 to 165.2 Bq/kg, with a mean value of 137.6 Bq/kg. Only the mean value of thorium recorded was higher than that given in the UNSCEAR report¹ for India. Comparatively low mean

RESEARCH COMMUNICATIONS

Table 1. Analytical results of the activity concentration (Bq/kg \pm 1 SD) of the major radionuclides in different geological formations

Sample no.	Formation	⁴⁰ K	²³⁸ U	²³⁵ U	²²⁶ Ra	²³² Th	²³⁰ Th	²¹⁰ Pb	¹³⁷ Cs
EK-02	Saryu	1652 \pm 37.9	129.4 \pm 5.4	8.3 \pm 1.8	55.6 \pm 2.3	96.0 \pm 3.1	1.7 \pm 4.2	0.1 \pm 0	BDL
EK-03	Saryu	1758 \pm 39.7	268.5 \pm 53.7	7.4	121.1 \pm 4.0	131 \pm 3.4	BDL	164.8 \pm 73.2	BDL
EK-04	Saryu	1710 \pm 38.8	203.4 \pm 43.5	5.5 \pm 3.0	90.4 \pm 1.6	102.4 \pm 1.4	4.1 \pm 2.5	130.3 \pm 71.2	BDL
EK-06	Saryu	985.6 \pm 23.8	143.2 \pm 29.8	NA	62.2 \pm 3.8	79.8 \pm 2.5	BDL	33.9 \pm 11.5	0.7 \pm 0.4
EK-07	Saryu	124.6 \pm 7.9	483.9 \pm 16.1	7.2 \pm 2.0	26.9 \pm 1.3	55.5 \pm 1.1	0.6 \pm 0.1	52.8 \pm 14.3	5.5 \pm 0.5
EK-09	Saryu	1212 \pm 35.8	261.8 \pm 53.6	7.7 \pm 3.2	79.6 \pm 4.5	135.9 \pm 12.5	6.8 \pm 5.8	BDL	1.5 \pm 0.4
EK-10	Saryu	910.4 \pm 22.6	234.9 \pm 8.1	8.6	147.4 \pm 20.7	114.7 \pm 4.4	3.0 \pm 5.0	28.6 \pm 11.5	0.7 \pm 0.4
EK-11	Saryu	743.9 \pm 15.6	940.6 \pm 27.7	12.1 \pm 3.2	35.7 \pm 1.3	62.2 \pm 3.3	BDL	1.3 \pm 0.2	BDL
EK-12	Saryu	1470 \pm 23.4	591.2 \pm 26.0	13.1 \pm 0.9	100.9 \pm 1.8	115.2 \pm 1.4	2.5 \pm 0.2	1.3 \pm 0.2	1.1 \pm 0.6
EK-13	Deoban	180.7 \pm 8.7	37.7 \pm 4.5	15.8 \pm 1.8	76.8 \pm 1.7	16.3 \pm 1.9	BDL	BDL	4.4 \pm 0.5
EK-14	Deoban	305.5 \pm 10.1	39.9 \pm 3.9	2.7 \pm 0.6	17.5 \pm 1.3	28.2 \pm 2.3	BDL	BDL	2.1 \pm 0.4
EK-15	Deoban	524.0 \pm 13.7	301.3 \pm 85	6.1 \pm 2.6	35.2 \pm 1.3	46.3 \pm 1.1	BDL	11.3 \pm 1.4	5.1 \pm 0.4
EK-16	Deoban	596.3 \pm 16.2	78.5 \pm 5.1	BDL	33.3 \pm 2.0	38.6 \pm 3.1	BDL	BDL	0.8 \pm 0.4
EK-17	Saryu	713.4 \pm 18.1	84.6 \pm 4.9	BDL	35.0 \pm 1.3	50.1 \pm 3.1	5.2 \pm 0.7	BDL	0.6 \pm 0.3
EK-18	Saryu	726.2 \pm 19.0	34.4 \pm 7.2	1.2 \pm 0.5	15.8 \pm 1.7	29.8 \pm 6.9	BDL	BDL	1.1 \pm 0.3
EK-19	Saryu	1330 \pm 31.5	93.1 \pm 20.2	BDL	36.0 \pm 1.4	40.8 \pm 2.2	BDL	BDL	BDL
EK-20	Saryu	866.1 \pm 16.8	1305.5 \pm 29.7	14.3 \pm 0.8	111.0 \pm 1.5	98.0 \pm 1.4	1.0 \pm 0.0	1.5 \pm 0.1	3.5 \pm 0.5
EK-21	Deoban	590.1 \pm 13.3	345.2 \pm 14.1	4.8 \pm 0.7	29.5 \pm 1.1	45.8 \pm 4.3	BDL	41.0 \pm 14.4	3.4 \pm 0.2
EK-22	Berinag	155.4 \pm 8.1	428.1 \pm 87.2	2.6 \pm 0.6	2.4 \pm 1.0	66.9 \pm 1.1	BDL	1.4 \pm 1.0	1.6 \pm 0.4
EK-23	Berinag	429.1 \pm 9.8	321.7 \pm 65.7	4.3 \pm 0.4	28.2 \pm 0.7	72.7 \pm 2.4	BDL	59.0 \pm 11.4	0.5 \pm 0.3
EK-25	Saryu	1537.0 \pm 34.9	182.7 \pm 38.0	11.7 \pm 1.2	60.1 \pm 1.6	124.1 \pm 5.3	BDL	BDL	BDL
EK-26	Saryu	802.7 \pm 16.2	383.2 \pm 29.7	5.6 \pm 2.5	42.3 \pm 1.3	65.1 \pm 2.7	0.2 \pm 0.0	60.5 \pm 20.5	BDL
EK-27	Saryu	1412.1 \pm 22.5	218.5 \pm 74.5	12.1 \pm 2.8	102.7 \pm 3.0	110.2 \pm 0.8	BDL	100 \pm 23.6	BDL
EK-28	Saryu	809.2 \pm 16.5	374.4 \pm 22.1	7.8 \pm 2.5	53.8 \pm 1.6	73.7 \pm 2.9	BDL	125.4 \pm 21.3	4.8 \pm 0.4
EK-29	Saryu	730.1 \pm 19.1	32.6 \pm 6.3	BDL	55.3 \pm 4.2	60.8 \pm 1.1	BDL	208.7 \pm 58.2	1.6 \pm 0.4
EK-31	Saryu	552.3 \pm 13.6	228.6 \pm 12.7	10.3 \pm 2.5	36.0 \pm 2.7	54.4 \pm 3.7	BDL	71.8 \pm 18.6	0.4 \pm 2.6
EK-34	Saryu	315.9 \pm 9.6	588.0 \pm 13.7	6.5 \pm 0.6	29.8 \pm 0.7	32.3 \pm 0.9	BDL	88.9 \pm 14.8	4.4 \pm 0.5
EK-35	Saryu	935.7 \pm 23.4	65.6 \pm 9.2	BDL	75.3 \pm 3.7	71.0 \pm 1.2	BDL	64.8 \pm 11.7	8.2 \pm 0.5
EK-39	Mandali	671.2 \pm 1.7	52.8 \pm 9.5	3.6 \pm 0.3	86.8 \pm 3.3	86.8 \pm 3.1	BDL	84.1 \pm 29.4	3.5 \pm 0.6
EK-40	Mandali	637.9 \pm 14.8	300.4 \pm 107.8	6.2 \pm 0.8	13.5 \pm 3.9	66.5 \pm 2.7	BDL	93.8 \pm 16.3	5.7 \pm 0.7
EK-41	Munsairi	709.3 \pm 16.1	807.1 \pm 237.7	13.2 \pm 0.8	103.6 \pm 1.4	77.8 \pm 1.3	3.1 \pm 0.3	96.2 \pm 21.2	BDL
EK-42	Munsairi	953.7 \pm 17.9	1070.5 \pm 26.9	8.0 \pm 0.8	64.7 \pm 3.0	92.8 \pm 4.8	BDL	151.4 \pm 21.2	1.8 \pm 0.5
EK-43	Munsairi	916.4 \pm 19.5	305.6 \pm 68.8	8.9 \pm 1.0	60.8 \pm 1.8	72.3 \pm 5.8	BDL	235.7 \pm 23.3	6.4 \pm 0.8
EK-44	Saryu	1144.5 \pm 22.9	383 \pm 14.3	11.0 \pm 2.0	122.6 \pm 2.6	136.3 \pm 4.2	5.8 \pm 1.2	136.2 \pm 6.1	1.2 \pm 0.2
EK-45	Saryu	1282.8 \pm 22.0	801.8 \pm 186.6	8.9 \pm 2.9	78.7 \pm 3.2	132.5 \pm 5.5	2.8 \pm 0.3	66.4 \pm 25.8	BDL
EK-46	Saryu	1423.5 \pm 15.2	347.8 \pm 27.8	15.7 \pm 3.1	186.9 \pm 4.7	130.4 \pm 3.3	BDL	128.8 \pm 16.7	2.6 \pm 0.4
EK-47	Saryu	1004.8 \pm 17.5	181.0 \pm 55.2	18.2 \pm 3.9	154.0 \pm 1.4	124.2 \pm 2.9	11.5 \pm 1.1	260.6 \pm 28.8	BDL

*BDL, Below detection limit.

Table 2. Statistical summary of radionuclides in soil samples collected from the eastern part of Kumaun Himalaya

	⁴⁰ K	²³⁸ U	²³⁵ U	²²⁶ Ra	²³² Th	²³⁰ Th	²¹⁰ Pb	¹³⁷ Cs	Ra _{eq}	Air Kerma rate (nGyh ⁻¹)	H _{ex}	H _{in}	Ambient dose equivalent rate (mSv y ⁻¹)
Mean	887.1	341.9	8.7	66.7	79.4	3.7	86.2	2.8	248.5	118.7	0.7	0.9	0.6
Median	809.2	268.5	8.0	60.1	72.7	3.0	71.8	2.0	234.8	112.7	0.6	0.8	0.6
S.D.	443.0	304.7	4.4	43.1	34.7	3.2	70.7	2.2	113.2	53.6	0.3	0.4	0.3
Standard error	72.8	50.1	0.8	7.1	5.7	3.0	13.1	0.4	18.6	8.8	0.1	0.1	0.0
Minimum	124.6	32.6	1.2	2.4	16.3	0.2	0.1	0.4	81.3	39.1	0.2	0.3	0.2
Maximum	1758.0	1305.5	18.2	186.9	136.3	11.5	260.6	8.2	483.0	226.8	1.3	1.8	1.1
No. of samples	37	37	29	37	37	13	29	26	37	37	37	37	37

value of radium in this formation is due to the absence of uranium-rich minerals like apatite, zircon, etc.

In the Deoban Formation radium activity was recorded to be 17.5–76.8 Bq/kg, with a mean value of 44.7 Bq/kg. ⁴⁰K was recorded as 180.7 to 935.7 Bq/kg, with a mean

value of 476.4 Bq/kg and ²³²Th activity in this formation varied from 16.3 to 71.0 Bq/kg, with a mean value of 38.8 Bq/kg. The radium equivalent activity in this formation was 81.3 to 248.9 Bq/kg, with a mean value 136.8 Bq/kg. The radium content in the soil samples of

Table 3. Statistical summary of the activity concentration of ^{226}Ra , ^{40}K and ^{232}Th (Bq/kg) with total radium equivalent activity (Bq/kg), (external and internal) hazard, total absorbed dose and effective dose rate in different geological formations in the eastern part of Kumaun Himalaya

Formation	^{40}K	^{226}Ra	^{232}Th	Ra_{eq}	Air kerma rate (nGy h^{-1})	H_{ex}	H_{in}	Ambient dose equivalent rate (mSv y^{-1})
Saryu Formation								
Mean	1082.7	78.7	92.3	294.1	140.7	0.8	1.0	0.7
Standard error	86.9	9.5	7.2	23.3	10.9	0.1	0.1	0.1
Median	1004.8	62.2	98.0	320.1	157.2	0.9	1.1	0.8
Minimum	124.6	15.8	29.8	114.3	53.7	0.3	0.4	0.3
Maximum	1758.0	186.9	136.3	483.0	226.8	1.3	1.8	1.1
Confidence level (95.0%)	180.3	19.7	14.9	48.2	22.7	0.1	0.2	0.1
Mandhali Formation								
Mean	654.6	50.2	76.7	210.2	100.1	0.6	0.7	0.5
Standard error	16.7	36.7	10.2	52.4	23.2	0.1	0.2	0.1
Median	654.6	50.2	76.7	210.2	100.1	0.6	0.7	0.5
Minimum	637.9	13.5	66.5	157.7	76.9	0.4	0.5	0.4
Maximum	671.2	86.8	86.8	262.6	123.2	0.7	0.9	0.6
Confidence level (95.0%)	211.6	465.7	129.0	666.4	294.6	1.8	3.1	1.4
Munsiari Formation								
Mean	859.8	76.4	81.0	258.4	122.8	0.7	0.9	0.6
Standard error	76.0	13.7	6.1	11.8	5.1	0.0	0.1	0.0
Median	916.4	64.7	77.8	269.5	126.0	0.7	0.9	0.6
Minimum	709.3	60.8	72.3	234.8	112.7	0.6	0.8	0.6
Maximum	953.7	103.6	92.8	270.8	129.6	0.7	1.0	0.6
Confidence level (95.0%)	327.1	58.8	26.4	50.8	22.1	0.1	0.3	0.1
Berinag Formation								
Mean	292.3	15.3	69.8	137.6	65.3	0.4	0.4	0.3
Standard error	136.9	12.9	2.9	27.6	13.2	0.1	0.1	0.1
Median	292.3	15.3	69.8	137.6	65.3	0.4	0.4	0.3
Minimum	155.4	2.4	66.9	110.0	52.1	0.3	0.3	0.3
Maximum	429.1	28.2	72.7	165.2	78.5	0.4	0.5	0.4
Confidence level (95.0%)	1738.8	163.9	36.8	350.5	167.9	0.9	1.4	0.8
Deoban Formation								
Mean	476.4	44.7	38.8	136.8	65.0	0.4	0.5	0.3
Standard Error	111.1	10.2	7.6	24.2	11.7	0.1	0.1	0.1
Median	420.0	34.3	35.5	124.2	58.2	0.3	0.5	0.3
Minimum	180.7	17.5	16.3	81.3	39.1	0.2	0.3	0.2
Maximum	935.7	76.8	71.0	248.9	118.9	0.7	0.9	0.6
Confidence level (95.0%)	285.5	26.3	19.7	62.1	29.9	0.2	0.2	0.1

this formation was higher than that in the Berinag Formation. However, the mean thorium value was less than that in the Berinag Formation. The dolomitic limestone was slightly phosphatic in this region⁴³. Precipitation of uranium takes place with phosphate; thus uranium and radium concentrations are always higher compared to other sedimentary rocks^{2,44}.

The Mandhali Formation of the same geological subgroup had radium activity ranging from 13.5 to 86.8 Bq/kg, with a mean value of 50.2 Bq/kg. ^{40}K was 637.9–671.2 Bq/kg, with a mean value of 654.6 Bq/kg. ^{232}Th activity was 66.5–86.8 Bq/kg, with a mean value of 76.7 Bq/kg. The radium equivalent activity in this formation varied from 157.7 to 262.6 Bq/kg, with a mean value of 210.2 Bq/kg. The rocks of the Mandhali Formation have fine

grain size, which offers high resistivity, i.e. it creates a compact structure of the upper layer of the soil and lack of channels accumulates the radionuclides inside. The low movement and accumulation of radionuclides in this Formation, gives a high mean value of ^{226}Ra , ^{232}Th and ^{40}K .

The Saryu Formation of Almora Group has high radionuclide content. ^{226}Ra activity in this formation varied from 15.8 to 186.9 Bq/kg, with a mean value of 78.7 Bq/kg, ^{40}K activity was 124.6–1758.0 Bq/kg, with a mean value of 1082.7 Bq/kg and ^{232}Th activity was 29.8–136.3 Bq/kg, with a mean value of 92.3 Bq/kg. The radium equivalent activity in this formation was 114.3–483.0 Bq/kg, with a mean value of 294.1 Bq/kg. The presence of high uranium in mineralized granite and

pegmatite are attributed to the ability of iron oxide to adsorb uranium from circulating solution or to the prevalence of oxidation conditions that cause the precipitation of U^{+} ion¹⁸. The high uranium content in fluorite may be attributed to fluorine ions, which forms a complex with uranium. These values are smaller than the radionuclide concentration in Wadi karim area of the eastern desert in Egypt and rocks comprise of post-tectonic granite and bostonite dykes¹⁸. The high radioactivity level in granite rocks, associated with pegmatites, is attributed to the presence of the radioactive minerals like thorianite, uranophane and allanite^{45,46}. The meso-to-epi grade para and orthogneisses, schist, calc silicate, marble, granites and their mylonitic equivalent forming the Munsiri Formation, constitute the root-zone rocks of the far-travelled detached thrust sheets (nappe and klippe) in the Lesser Himalaya.

The ²²⁶Ra activity concentration in Munsiri Formation varied from 60.8 to 103.6 Bq/kg, with a mean value of 76.4 Bq/kg, ⁴⁰K was from 709.3 to 953.7 Bq/kg, with a mean value of 859.8 Bq/kg and ²³²Th activity was 72.3 to 92.8 Bq/kg, with a mean value of 81.0 Bq/kg. The radium equivalent activity in this formation was 234.8 to 270.8 Bq/kg, with a mean value of 258.4 Bq/kg. This is less than 370 Bq/kg, which is acceptable for safe use of the rocks and soil for construction purpose¹².

The distribution of other radionuclides like ¹³⁷Cs and ²¹⁰Pb is not directly related with the measurement of the air kerma dose rate and ambient dose equivalent, but ¹³⁷Cs is considered to be the most important isotope from the point of view of the external gamma dose. The concentration of ²¹⁰Pb was found to be consistently higher than that of ¹³⁷Cs at all sampling sites (locations). ¹³⁷Cs content varied between 0.4 and 8.2 Bq/kg, with a mean value of 2.8 Bq/kg in the study area. The highest and lowest ¹³⁷Cs content was attributed to the same formation, which shows that the different geological formations are not responsible for ¹³⁷Cs variation. ²¹⁰Pb activity in the soil also affects ²¹⁰Po in the dwellings, which is used for the retrospective assessment of radon indoors. The results of ²¹⁰Pb may be used as a reference for any retrospective study in the near future in the area. The ²¹⁰Pb activity varied between 0.1 and 260.3 Bq/kg, with a mean value of 86.2 Bq/kg. The lowest and highest values were recorded in the Saryu Formation of the study area, but at different locations.

Some interesting trends in the ²²⁶Ra/²³⁸U concentration were recorded with respect to different geological formations. The ratio decreased slightly as we moved from Berinag to Deoban and Saryu formations. The same declining trend was also observed for the ²³⁵U/²³⁸U ratio, whereas the ²³⁸U/²³²Th ratio did not show any definite pattern. The results from ratio analysis will be helpful to explain equilibrium conditions at different locations. Extreme disequilibrium among ²³⁸U : ²³⁰Th : ²²⁶Ra (#EK20; Table 1) in Champawat region is due to the granitic rocks

of the concordant Champawat body, which are magmatic in origin as indicated by complexly twined and zoned plagioclases⁴⁷. The rocks of this region are comagmatic (the individual types reflecting varied physical conditions of emplacement), and are bound to systematic progressive changes in the proportion of N_2O , K_2O , CaO , Fe_2O_7 , FeO (ref. 21). These complex chemical reactions may have resulted in the disequilibrium of the radionuclides.

The average values distributed over the study area were computed for correlation coefficient between radionuclides (Table 4). Strong correlation was observed between ⁴⁰K and ²²⁶Ra (0.6), ⁴⁰K and ²³²Th (0.7), ²³⁵U and ²²⁶Ra (0.8) as well as ²²⁶Ra and ²³²Th (0.7). A weak negative correlation was observed between ⁴⁰K and ²³⁰Th (-0.2), ²³⁸U and ²³⁰Th (-0.3), ²²⁶Ra and ²³⁰Th (-0.4) as well as ²³²Th and ²³⁰Th (-0.5). The negative correlation shows that the radionuclide concentrations are associated with different chemical and geological properties of the elements. The different contents of clay and sand in soil samples also contribute to the correlation coefficient, with micro-cracks, fractures and mobility characteristic of the radionuclides in geological medium. Uranium chemistry changes with reducing and oxidizing environment, but radium chemistry is relatively simple as it behaves like the other alkaline earth metals⁴⁸.

The air-absorbed dose rate at a height of 1 m above the ground level and other radiological effects were calculated when the soil samples were used as construction material on a local scale. These results are also important for the purpose of environmental protection studies, since the local soil in the hilly areas is used for different purposes in the mud houses, mainly for flooring and labelling the walls. The building materials act as a source of radiation and also shield against outdoor radiation⁴⁰. Massive houses were made using stone, soil and wood in the hilly areas. The fraction of radiation emitted by the soil will contribute to the total radiation level indoors, and the radiation emitted by sources outdoor is efficiently absorbed by the wall. Consequently, the dose rate indoors will be more according to the radionuclide content in the soil used for the construction. The fluxes of the ionizing radiation in the indoor air will increase as a consequence of the soil having more radionuclides. The average calculated absorbed dose rate varied from 39.1 to 226.8 nGy h⁻¹, with a mean value of 118.7 nGy h⁻¹. The average absorbed dose rate in air was reported as 56 nGy h⁻¹ by UNSCEAR¹ for India. The recorded value in study area is nearly twice the Indian average and thus a detail study in necessary and important for health hazard effects to the people living there. The ultimate use of the activity measured in the soil samples is to measure the radiation dose delivered externally in the form of gamma dose. The external hazard indexes (H_{ex}) were calculated from 0.2 to 1.3, with a mean value of the 0.7; the calculated average values are less than the acceptable value (1.5). These radionuclides are a source of radon (²²²Rn) and its

Table 4. Correlation coefficient between different radionuclides

	⁴⁰ K	²³⁸ U	²³⁵ U	²²⁶ Ra	²³² Th	²³⁰ Th	²¹⁰ Pb	¹³⁷ Cs
⁴⁰ K	1							
²³⁸ U	0.0	1						
²³⁵ U	0.3	0.3	1					
²²⁶ Ra	0.6*	0.1	0.8*	1				
²³² Th	0.7*	0.2	0.4	0.7*	1			
²³⁰ Th	-0.2	-0.3	0.5*	-0.4	-0.5	1		
²¹⁰ Pb	0.2	-0.3	0.3	0.3	0.3	0.9*	1	
¹³⁷ Cs	-0.2	0.1	0.1	-0.1	-0.2	-0.4	0.2	1

*Shows significant correlation coefficient ($P = 0.95$).

radioactive progeny. The internal exposure by radon and its progeny is controlled by the internal hazard index H_{in} . H_{in} less than 1 is suggested for materials used for house construction. H_{in} of 1.8 was calculated for the soil collected from igneous rocks of the Saryu Formation. The observed higher value of the internal hazard index in the Saryu Formation was due to the presence of radioactive minerals in the rocks of this formation. The annual effective dose rate of the study area varied from 0.2 to 1.1 mSv y^{-1} , with a mean value of 0.6 mSv y^{-1} . According to the recent regulation issued by the European Union in 1999 (ref. 49), building materials should be exempted from all construction purposes if the excessive gamma radiation due to them causes an increase in the annual effective dose received by an individual by a maximum value of 0.3 mSv.

High occurrences of radionuclides are associated with mylonitized granite gneiss, augen gneiss, garnetiferous mica schist and micaceous weathered quartzite, and tectonically emplaced bodies of granite and granodiorite of Saryu and Munsiri formations. Presence of uranium mineralization in the shear zone associated with different thrusts and faults may be responsible for high radioactivity in the study area. The diverse lithology and associated complex tectonic features also contribute to radioactivity in the environment. The observed results show some strong disequilibrium conditions in the study area with respect to the oxidizing and reducing environment. Based on this study on radium equivalent activity, absorbed dose rate, external and internal hazard indices and annual effective dose rate, it is recommended that radiometric survey is necessary before choosing raw materials for construction purposes and location of houses in the Himalayan region. Use of soil and rocks from these locations needs careful regulation to reduce the radiation levels into the surroundings. These results will also provide the baseline data for the future with respect to geophysical and geomorphologic changes in the study area.

1. UNSCEAR, Sources and effects of ionizing radiation (without scientific annexes), United Nations Scientific Committee on the Effect of Atomic Radiation, 2000, p. 6.

2. ICRP, *Annals of ICRP 23, Protection Against ²²²Rn at Home and at Work*, Pergamon Press, Oxford, International Commission for Radiation Protection, Publication No. 60, 1993.
3. Ramola, R. C., Choubey, V. M., Prasad, Y., Prasad, G. and Bartarya, S. K., Variation in radon concentration and terrestrial gamma radiation dose rate in relation to the lithology in southern part of Kumaun Himalaya, India. *Radiat. Meas.*, 2006, **41**, 714–720.
4. Mason, B. and Moore, C. B., *Principle of Geochemistry*, John Wiley, New York, 1982, 4th edn, p. 344.
5. Rogers, J. J. W. and Adams, J. A. S., Uranium. In *Handbook of Geochemistry*, (ed. Wedepohl, K. H.), Springer-Verlag, Heidelberg, 1969, p. 92.
6. Edsfield, C., The radium distribution in some Swedish soils and its effects on radon emanation. PhD thesis submitted to Division of Engineering Geology, Royal Institute of Technology Stockholm, 2001, pp. 1–52.
7. Guthrie, V. A. and Kleeman, J. D., Changing uranium distributions during weathering of granite. *Chem. Geol.*, 1986, **54**, 113–126.
8. Waite, T. D. and Payne, T. E., Uranium transport in the subsurface environment, Koongarra, a case study. In *Metals in Groundwater* (eds Allen Herbert, E. et al.), Chelsea, 1993, pp. 349–410.
9. Langmuir, D. and Herman, J. S., The mobility of thorium in natural waters at low temperatures. *Geochim. Cosmochim. Acta*, 1980, **44**, 1753–1766.
10. Gundersen, L. C. S., Schumann, R. R., Otton, J. K., Dubiel, R. F., Owen, D. E. and Dickinson, K. A., Geology of radon in United States. In *Geologic Controls on Radon Special Paper 271* (eds Gates, A., Alexander, E. and Gunderson, L. C. S.), Geological Society of America, 1982, pp. 1–16.
11. Molinari, J. and Snodgrass, W. J., The chemistry and radiochemistry of radium and other elements of the uranium and thorium natural decay series. In *The Environmental Behaviour of Radium*, IAEA Technical Reports Series No. 310, International Atomic Energy Agency, Vienna, 1990, vol. 1, pp. 11–56.
12. OECD, Exposure to radiation from the natural radioactivity in building materials. Nuclear Energy Agency, Organization for Economic Cooperation Development, Paris, France, 1979.
13. Radhakrishna, A. P., Somashekarappa, H. M., Narayana, Y. and Siddappa, K., A new natural background radiation area on the southwest coast of India. *Health Phys.*, 1993, **65**, 390–395.
14. Quindos, L. S., Fernandez, P. I., Soto, J., Rodenas, C. and Gomez, J., Natural radioactivity in Spanish soils. *Health Phys.*, 1994, **66**, 194–200.
15. Choubey, V. M., Bisht, K. S., Saini, N. K. and Ramola, R. C., Relation between soil gas radon variation and different lithotectonic units of Garhwal Himalaya, India. *Appl. Radiat. Isot.*, 1999, **51**, 587–592.
16. Singh, S., Rani, A. and Mahajan, R. K., ²²⁶Ra, ²³²Th and ⁴⁰K analysis in soil samples from some areas of Punjab and Himachal

- Pradesh, India using gamma ray spectrometry. *Radiat. Meas.*, 2005, **39**, 431–439.
17. Mireles, F., Davila, J. I., Quirino, L. L., Lugo, J. F., Pinedo, J. L. and Rios, C., Natural soil gamma radioactivity levels and resultant population dose in the cities of Zacatecas and Guadalupe, Zacatecas, Mexico. *Health Phys.*, 2003, **84**, 368–372.
 18. El-Arabi, A. M., ²²⁶Ra, ²³²Th and ⁴⁰K concentrations in igneous rocks from eastern desert, Egypt and its radiological implication. *Radiat. Meas.*, 2007, **42**, 94–100.
 19. Choubey, V. M., Radon measurements in soil and water and its relation with geology, Garhwal Himalaya. In Proceeding Volume of 7th Tohwa International symposium 'Radon and Thoron in the Human Environment (eds Katase, A. and Shimo, M.), Fukuoka, Japan October 1997, World Scientific, 1998, pp. 193–198.
 20. Raina, B. N. and Dungrakoti, B. D., Geology of the area between Nainital and Champawat, Kumaun Himalaya, Uttar Pradesh. *Himalayan Geol.*, 1975, **5**, 1–27.
 21. Valdiya, K. S., *Geology of Kumaun Lesser Himalaya*, WIHG Publication, Dehra Dun, 1980, p. 291.
 22. Valdiya, K. S., Neotectonic activity in the Himalayan belt. In Proceedings International Symposium on Neotectonics in South Asia. Survey of India, Dehra Dun, 1986, pp. 248–267.
 23. Bartarya, S. K. and Valdiya, K. S., Landslides and erosion in the catchment of the Gaula River, Kumaun Lesser Himalaya, India. *Mt. Res. Dev.*, 1989, **9**(4), 405–419.
 24. Papachristodoulou, C. A., Assimakopoulos, P. A., Patronis, N. E. and Ioannides, K. G., Use of HPGe gamma ray spectrometry to assess the isotopic composition of uranium in soils. *J. Environ. Radioact.*, 2003, **64**, 195–203.
 25. Karangelos, D. J., Anagnostakis, M. J., Hinis, E. P., Simopoulos, S. E. and Zunic, Z. S., Determination of depleted uranium in environmental samples by gamma-spectroscopic techniques. *J. Environ. Radioact.*, 2004, **76**, 295–310.
 26. Tzortzis, M. and Tsertos, H., Determination of thorium, uranium and potassium elemental concentrations in surface soils in Cyprus. *J. Environ. Radioact.*, 2004, **77**, 325–338.
 27. Shanbhag, A. A., Sartandel, S. J., Ramachandran, T. V. and Puranik, V. D., Natural radioactivity concentrations in beach sands of Ratnagiri coast, Maharashtra. *J. Assoc. Environ. Geochem.*, 2005, **8**, 304–308.
 28. Strachnov, V., Valkovic, V., Zeisler, R. and Dekner, R., Report on the intercomparison run IAEA-314: ²²⁶Ra, Th and U in stream sediment. AQCS/IAEA, Vienna, Austria, 1991.
 29. Hamby, D. M. and Tynybekov, A. K., Uranium, thorium and potassium in soils along the shore of lake Issyk-Kyol in the Kyrghyz Republic. *Environ. Monit. Assess.*, 2002, **73**, 101–108.
 30. Degerlier, M., Karahan, G. and Ozger, G., Radioactivity concentrations and dose assessment for soil samples around Adana, Turkey. *J. Environ. Radioact.*, 2008, **99**, 1018–1025.
 31. Petropoulos, N. P., Anagnostakis, M. J. and Simopoulos, S. E., Photon attenuation, natural radioactivity content and radon exhalation rate of building materials. *J. Environ. Radioact.*, 2001, **61**, 257–269.
 32. Strachnov, V., Valkovic, V., Zeisler, R. and Dekner, R., Report on the intercomparison run IAEA-312: ²²⁶Ra, Th and U in soil. AQCS/IAEA, Vienna, Austria, 1991.
 33. Currie, L.A., Limits for qualitative detection and quantitative determination. *Ann. Chem.*, 1968, **40**, 586–593.
 34. Yu, K. N., Guan, Z. J., Stoks, M. J. and Young, E. C., The assessment of natural radiation dose committed to the Hong Kong people. *J. Environ. Radioact.*, 1992, **17**, 31.
 35. Tufail, M., Ahmad, N., Mirza, S. M., Mirza, N. M. and Khan, H. A., Natural radioactivity from the building materials used in Islamabad and Rawalpindi, Pakistan. *Sci. Total Environ.*, 1992, **121**, 283–291.
 36. Quindos, L. S., Fernandez, P. L. and Soto, J., Building materials as source of exposure in houses. In *Indoor Air 87* (eds Seifert, B. and Esdorn, H., Institute of Water, Soil and Air Hygiene, Berlin, 1987, vol. 2, p. 365.
 37. Cottens, E., Actions against radon at the international level. In Proceedings, Symposium on SRBII, Journee Radon, Royal Society of Engineers and Industrials of Belgium, Brussels, 17 January 1990.
 38. Jacob, P., Paretzke, H. G., Rosenbaum, H. and Zankl, M., Effective dose equivalents for photon exposure from plane sources on the ground. *Radiat. Prot. Dosim.*, 1986, **14**, 299–310.
 39. Leung, K. C., Lau, S. Y. and Poon, C. B., Gamma radiation dose from radionuclides in Hong Kong soil. *J. Environ. Radioact.*, 1990, **11**, 279–290.
 40. UNSCEAR, Exposure from natural sources of radiation. United Nations, United Nations Scientific Committee on the Effects of Atomic Radiation, New York, 1993.
 41. UNSCEAR, Sources and biological effects. United Nations Scientific Committee on the Effects of Atomic Radiation, Report to the General Assembly with Annexes, United Nations Sales Publication E.82.IX.8, New York, 1982.
 42. Cuney, M., LeFort, P. and Wangege, Z., *Geology of Granites and their Metallogenetic Relations*, Science Press, Moscow, 1987, pp. 852–873.
 43. Valdiya, K. S., A new phosphatic horizon in the late Precambrian Calc Zone of Pithoragarh, Kumaun Himalaya. *Curr. Sci.*, 1969, **38**, 415–416.
 44. Akerblom G. and Wilson C., Radon gas – a radiation hazard from radioactive bedrock and building materials. *Bull. Int. Assoc. Eng. Geol.*, 1982, **23**, 51–61.
 45. Omran, A., Petrochemical studies and potentiality of uranium–thorium occurrences in Gabal Um Taghir El-Tahtani area with emphasis on the granitic rocks, central Eastern Desert, Egypt. Ph D thesis Geological, Ain Shams University, 2005.
 46. Anjos, R. et al., Natural radionuclide distribution in Brazilian commercial granites. *Radiat. Meas.*, 2005, **39**, 245–253.
 47. Valdiya, K. S., A study of Champawat Granodiorite and associated metamorphics of the Lohaghat subdivision, District Almora, with special reference to petrography and petrogenesis. *Indian Mineral.*, 1962, **3**, 6–37.
 48. Edsfeldt, C. and Fernlund, J., Difference in radium and uranium distribution in quaternary deposits, Proc. of the Int. Radon Symposium, Wisconsin, USA, 22–25 October 2000, pp. 2.0–2.10.
 49. EC, European Commission report on radiological protection principles concerning the natural radioactivity of building materials. Radiation Protection Publication No. 112, 1999.

ACKNOWLEDGEMENTS. We thank the Board of Research in Nuclear Sciences, Department of Atomic Energy, Government of India for providing financial support in the form of a project. We also thank the Director, Wadia Institute of Himalayan Geology, Dehradun, for providing facilities to carry out this work. V.M.C. thanks FNR, Luxembourg for providing financial support to visit Luxembourg University under a joint collaborative research programme. The contribution of scientific data by late Dr Yogesh Prasad will be remembered.

Received 8 December 2009; revised accepted 22 November 2010